The *Spitzer* First Look Survey Ecliptic Plane Component: Asteroids and Zodiacal Background

V. S. Meadows[1], B. Bhattacharya, W. T. Reach, C. Grillmair, A. Noriega-Crespo, E. L. Ryan, S. R. Tyler, L. M. Rebull

Spitzer Science Center, California Institute of Technology, Pasadena, CA 91125

vsm@ipac.caltech.edu

J. D. Giorgini

Jet Propulsion Laboratory, California Institute of Technology

and

J. L. Elliot

Department of Earth, Atmospheric and Planetary Sciences, Massachusetts Institute of Technology

ABSTRACT

The *Spitzer* First Look Survey (FLS) provided an initial characterization of the infrared sky at *Spitzer* wavelengths and sensitivities. The Ecliptic Plane Component (EPC) of the FLS concentrated on two 0.13 $\deg^2$, fields at a solar elongation of 115°, and ecliptic latitudes (β) of 0° and +5°. The FLS-EPC explored the small asteroid counts at 8 and 24 μm, with a detection limit down to ~ 0.08 mJy and 0.4 mJy, respectively; and a completeness limit almost twice as deep as the 8μm equivalent flux density of the previous deepest MIR survey. The FLS-EPC also provided initial characterization of the zodiacal light near the ecliptic plane. Fourteen known and 21 unknown asteroids were identified, and asteroids detected at both wavelengths displayed similar 8 to 24 μm flux ratios of ~ 0.1. Comparing number counts for the $\beta = 0°$ and +5° fields indicate a slower than anticipated drop-off when compared with predicted scale heights. This may indicate an increase in the asteroid scale height due to the presence of higher inclination objects in the small population sampled by *Spitzer*. The measured zodiacal light background was found to be within 5% of *Spitzer* model predictions at 24 μm.

---

[1]also NASA Astrobiology Institute

Subject headings: asteroids: general

1. Introduction

The First Look Survey[2] (FLS) was envisaged in 1999 to provide a first characterization of the sky at the mid-infrared wavelengths and typical sensitivities achievable with the *Spitzer Space Telescope* (Werner et al., 2004). The goal of the Ecliptic Plane Component (FLS-EPC) of the FLS was to characterize main belt asteroids and the zodiacal light as a function of distance from the ecliptic plane. Main belt asteroids between 2 and 4 AU were targeted to determine number counts as a function of observed brightness, and ecliptic plane scale heights, for objects with diameters down to < 1 km. This survey, which attained 0.08 mJy at 8 μm, is potentially sensitive to asteroids > 0.5 km in diameter, as was the visible Sloan Digital Sky Survey (Ivezić, 2001) but is also ~ 2 times more sensitive than previous mid-infrared (MIR) surveys, allowing us to probe the relatively unknown population of sub-km main belt asteroids in the MIR. The most sensitive previous survey at MIR wavelengths, the ISO deep asteroid search, detected asteroids down to 0.6 mJy at 12 μm, which is an 8 μm equivalent flux density of 0.16mJy (Tedesco and Desert, 2002; Tedesco, Cellino and Zappala, 2003). Although not reported here, supporting, contemporaneous ground-based visible observations that included the FLS-EPC asteroid sample were also taken to provide asteroid sizes, orbits and distances; these results will be reported in Tedesco et al., 2004 (in prep).

The FLS-EPC also investigated the natural MIR background brightness for *Spitzer* in the ecliptic plane. The sensitivity of *Spitzer* is background-limited, and dominated by zodiacal light at all but the longest wavelengths and lowest galactic latitudes. Although not optimized for absolute background measurements, *Spitzer's* short-wavelength Infrared Array Camera (IRAC) (Fazio et al., 2004) can provide absolute photometry relative to the brightness of a dark sky patch. At 24 μm, the longer-wavelength Multiband Imaging Photometer for *Spitzer* (MIPS) (Rieke et al., 2004) provides accurate absolute photometry of the zodiacal light.

2. Observations

All observations described here were taken with the *Spitzer* Space Telescope, using 14.3 hrs of Director's Discretionary Time. The observations were executed on the spacecraft

[2] http://ssc.spitzer.caltech.edu/fls

between UTC 2004 January 21 02:35:22 - 20:57:13.

The FLS-EPC consisted primarily of two 0.13 deg^2 fields ($10' \times 48'$) which were centered at a solar elongation as seen from *Spitzer* of 115°, in the hemisphere that contained the Earth, and at $\beta = 0°$ and $+5°$. In J2000 celestial coordinates, this corresponds to field centers of RA=12:03:22.03, Dec= -00:21:53.8 for the $\beta = 0°$ field, and RA=12:11:20.10, Dec= +04:13:18.7 for the $\beta = +5°$ field, as viewed from *Spitzer*. Both fields were observed with IRAC and MIPS, each of which take simultaneous observations at multiple wavelengths. However, asteroids are most easily detected at 8μm (IRAC) and 24μm (MIPS) with *Spitzer*, as their thermal emission peaks near 20 μm. MIPS was also used to observe a single $\beta = 0-6°$ continuous strip running through the two latitude fields.

To detect asteroid motion, each IRAC field was observed at 3 epochs separated by 70 minutes. Although asteroids are typically brighter at 24μm, IRAC observations at 8 μm were chosen for detection, due to this instruments higher sensitivity and smaller pixel size. A single epoch MIPS slow-scan observation of each field was also taken to provide color information for asteroids detected by IRAC. Although the anticipated spread of apparent asteroid motion in our fields encompassed retrograde motion, the majority of asteroids were predicted to be moving in a prograde direction as viewed from Spitzer. Therefore, to maximize the probability of detection by both instruments, the MIPS observations covered the IRAC field, and extended 50% of the IRAC field width in positive RA, the prograde direction for main belt asteroids. The observations were scheduled on an IRAC/MIPS instrument campaign boundary, and the first MIPS observation after the 3.5 hr instrument changeover was executed 10hrs and 7 minutes after the start of the IRAC observations. The exposure time was 120 s per pointing for the IRAC (8μm) observations and 200 s per pointing for the MIPS (24 μm) scan map observations for each latitude field. The 6° MIPS strip through the two fields was a fast scan with 15 s per pointing. Details of the observing plan can be found on the *Spitzer* web site[3]. The Astronomical Observing Requests (AORs) used for this program can be examined using the *Spitzer* Observation Planning Tool (SPOT), with the File:View Program function and Program ID 98.

All data were processed with the standard *Spitzer* data reduction pipelines, which produced individual observing frames that were corrected for instrumental and spacecraft effects. These reduced frames, or Data Collection Events (DCEs) were combined using the post-pipeline mosaicing software to create a single map for each instrument, field and epoch of observation.

[3]http://ssc.spitzer.caltech.edu/fls/eclip

2.1. Asteroid Finding Techniques

For each of the latitude fields, we colored and coadded the IRAC 8 μm mosaics of the three epochs to create a composite Red, Green, and Blue (RGB) image, which was then examined by eye (Figures 1 and 2). In this RGB image, fixed sources appeared white, and moving targets were seen as red-green-blue quasi-linear sequences of sources. Typical S/N for detected sources was > 10. Our fastest apparent motion was $26''$/hr, and the slowest apparent motion was $3.6''$/hr. Simulations of the apparent motion of main belt asteroids at the solar elongation observed by *Spitzer* suggest that only 5% of our sample had apparent motions less than this (Brooke, 2003)[4].

However, to more objectively study the asteroid distributions, and to potentially identify more objects at lower S/N, we also used the IRAF implementation of the DAOPHOT/ALLSTAR (Stetson 1994) stellar photometry packages to detect and measure sources. All objects down to 3σ above the noise were detected within the inner $0.09\,\mathrm{deg}^2$ of each 8 μm mosaic (where uniform overlap of frames ensures similar noise levels) and photometry was obtained with the PSF-fitting ALLSTAR routine. The three lists of measured sources in each field were searched for objects which moved between epochs at uniform rates between 2-$50''$/hr, and in a quasi-linear fashion ($< 5^\circ$ of deviation from a straight line connecting all three detections).

3. Results

3.1. *Spitzer* Observations of Known Asteroids: 8 and 24μm fluxes

Using JPL Horizons[5] predictions, we identified 11 known asteroids in the IRAC 0° field, and 4 in the IRAC +5° field. Using SPOT, we overplotted their predicted time-dependent apparent position on the *Spitzer* MIPS data and were able to identify MIPS counterpart observations for all of the 15 known asteroid IRAC detections. However, two of these were sufficiently close to a map boundary that accurate photometry could not be obtained, and one landed on a bright background galaxy. The measured thermal fluxes for the known asteroids for which reliable photometry was obtained at both 8 and 24 μm are given in Table 1.

---

[4]http://ssc.spitzer.caltech.edu/documents/asteroid_memo.pdf

[5]http://ssd.jpl.nasa.gov/horizons.html

3.2. Asteroid Counts

Using the RGB technique with the $8\,\mu$m data, and assuming Poisson noise statistics, we were able to identify 18(±4.2) sources in the $\beta = 0°$ field and 16(±4) sources in the $\beta = +5°$ fields. The faintest of these sources have $8\,\mu$m fluxes close to 0.08 mJy, and were detected with a S/N∼10, in both fields. Using the automated detection technique, and to a flux limit > 0.05mJy, where our point-source completion tests suggest that we are 60% complete, we found 9(±3) sources in the inner 0.09 deg^2 of the 0° field and 10(±3.2) sources in the inner 0.09 deg^2 of the 5° field. This corresponds to equivalent counts in the 0.13 deg^2 field of 14(±4.5) and 15.5(±5.0) respectively.

Our measured asteroid counts as a function of area are shown in Table 2. Although the list of RGB sources is larger than the DAOPHOT list to similar flux limits, and encompasses the non-uniform noise regions at the mosaic edges, we used the automatically detected sources to enable more direct, objective estimates of completeness. Using standard artificial star tests, we determined that our detection completeness remains above 90% down to 0.1 mJy, and then drops quickly to 50% at 0.07 mJy, and to zero at 0.04 mJy. The estimated completeness fraction in the 5° field is slightly higher than that of the 0° field at any given flux level due to the reduction of the zodiacal light, but the difference is $< 2 - 3\%$.

If we consider asteroids observed down to flux levels of 0.1 mJy, where we have $> 90\%$ completeness, our uncorrected observed counts correspond to 134±31 asteroids per deg^2 at $\beta = 0°$, and 108±29 asteroids per deg^2 at $\beta = +5°$ latitude. However, for estimates of the total population, these observed counts have been increased by 5% to account for asteroids moving too slowly to be detected in our observations, and then increased by 10% to correct for detection incompleteness at 0.1 mJy. The corrected counts are shown in Table 2.

In Figure 3 we plot the luminosity functions, both before and after completeness correction, for the 0° and 5° fields. Adopting a power law for the surface density distribution $\propto f^{-\alpha}$, we use the completeness corrected counts to measure power law slopes $\alpha = 0.24 \pm 0.4$ and $\alpha = 0.61 \pm 0.4$ for the 0° and 5° fields, respectively. Whereas there is a suggestion in both the automatic and RGB detections that there are more faint asteroids in the 5°field, within the measurement errors the measured slopes are consistent with being identical. Applying a two-tailed Kolmogorov-Smirnoff test, we cannot reject the hypothesis that the two distributions came from the same parent population at the 16% probability level. If we then combine the power laws for the two fields we obtain $\alpha = 0.42 \pm 0.3$.

3.3. Zodiacal Background in the Ecliptic Plane

To obtain the total measured background in our frames, we added back the sky-dark that was removed from the data in the IRAC pipeline. We have compared our data with the SPOT background model (derived from the COBE/DIRBE data (Reach, 2000)[6]). The total background brightness measured at 8 μm was 36% brighter than model predictions. Using the MIPS fast scan strip from $\beta = 0$ to $+6°$, we measured the background at 24 μm, as provided in the standard pipeline data products. The observed background was 5% brighter than the 24 μm SPOT model prediction. Although background measurements were simultaneously made at other wavelengths with IRAC and MIPS, these data were not analyzed for this publication.

4. Discussion

4.1. Asteroids

The ratio of $F_{8\mu m}/F_{24\mu m}$ for all asteroids with reliable photometry at both wavelengths is 0.11 ± 0.02, implying that the asteroids have similar temperatures and are members of the main belt. Our observed number counts are compared with the Brooke (2003) and the Statistical Asteroid Model (SAM) predictions in Table 2. A significant difference between the two models is that SAM explicitly models the effect of both field asteroids and asteroid families on counts. SAM predicts that the proportions of individual asteroid families among the asteroids in a given field are strongly dependent on ecliptic latitude and substantially different for observations at visual versus infrared wavelengths.

To sensitivities of 0.1 mJy at 8 μm, our observed number counts are lower than the nominal values predicted by Brooke (2003), although within that model's predicted factor of 3 error. Our counts are consistent with the extrapolated ISO asteroid counts (Tedesco and Desert, 2002) and those predicted by the SAM model, and anchored to the ISO asteroid counts (Tedesco et al., 2003, submitted; Tedesco and Desert, 2002). The Brooke model also predicts that the ratio of asteroids detected to 0.1mJy in the +5° field to that in the 0° field is 0.5. SAM predicts 0.6 ± 0.1, in part due to the inclusion of high-inclination, low-albedo asteroid families, which increases the population of asteroids observed at IR wavelengths at higher ecliptic latitudes. The observed FLS-EPC ratio is 0.8. However, significant Poisson errors due to our relatively small sample indicate that this ratio could be as high as 1.4, or

[6]http://ssc.*Spitzer*.caltech.edu/documents/background/

as low as 0.5. Due to small number statistics, the FLS-EPC number counts are therefore not conclusive evidence for a different luminosity function with ecliptic latitude, or for a more slowly decreasing population distribution with increased ecliptic latitude, although they are suggestive of this. Further observations are required to get a more conclusive picture of asteroid scale height behavior at these wavelengths and flux limits, and to determine revised asteroid counts at ecliptic latitudes poleward of $\beta = 5°$.

4.2. Zodiacal Light

Although the best way to obtain accurate measurements of the zodical light with *Spitzer* will be the yet-to-be-commissioned MIPS Total Power Mode (TPM), we attempted first-order determinations of the absolute brightness of the ecliptic background at IRAC and MIPS wavelengths. For the 24 μm data, we obtained extremely good agreement between the observed background and the SPOT background model. The 5% correlation is well within both the absolute calibration uncertainty and the possible color-correction from the stellar calibrators to the much redder zodiacal light. Although the 8μm was 36% brighter than model predictions we believe this is consistent with known intrinsic variations in the zodiacal light background as a function of viewing geometry.

5. Conclusions

This survey, although a "First Look", was nonetheless the deepest MIR asteroid search to date. We find that asteroids are a significant component of *Spitzer* observations at low ecliptic latitudes, especially in MIPS 24 μm data, and future *Spitzer* observers should factor this in to planned observations near the ecliptic plane. We find that the asteroid counts are consistent with the SAM model predictions (Tedesco et al., 2004), which is our current best predictor of asteroid counts in *Spitzer* data. These data suggest that asteroid counts may not fall off with increasing ecliptic latitude as rapidly as some models predict, which would imply a higher inclination distribution in the smaller asteroid population that *Spitzer* detects. Further observations are needed, especially at higher latitudes, to determine where this distribution turns over. We get very good agreement between the *Spitzer* background model and observed brightnesses at 24μm, and a reasonable agreement at 8 μm, consistent with observed instrinsic variability in the zodiacal background.

We are grateful to S. Ramirez for providing fixed target catalog source detections for the MIPS fields. This analysis used the Horizons database, supported by the JPL Solar System

Dynamics group. This work is based on observations made with the *Spitzer* Space Telescope, which is operated by the Jet Propulsion Laboratory, California Institute of Technology under NASA contract 1407. Support for this work was provided by NASA through an award issued by JPL/Caltech.

REFERENCES

Fazio et al. 2004, ApJS, this volume.

Ivezić, Ž. and 32 others, 2001, AJ,122, 2749

Reach, W. T., Franz, B. A., & Weiland, J. L. 1997, Icarus, 127, 461

Reike et al. 2004, ApJS, this volume.

Stetson, P. B. 1994, PASP, 106, 250

Tedesco, E. F., & Desert,F.-X. 2002, AJ, 123, 2070

Tedesco, E. F., Cellino, A. & Zappala, V., 2004, AJ, submitted.

Werner et al. 2004, ApJS, this volume.

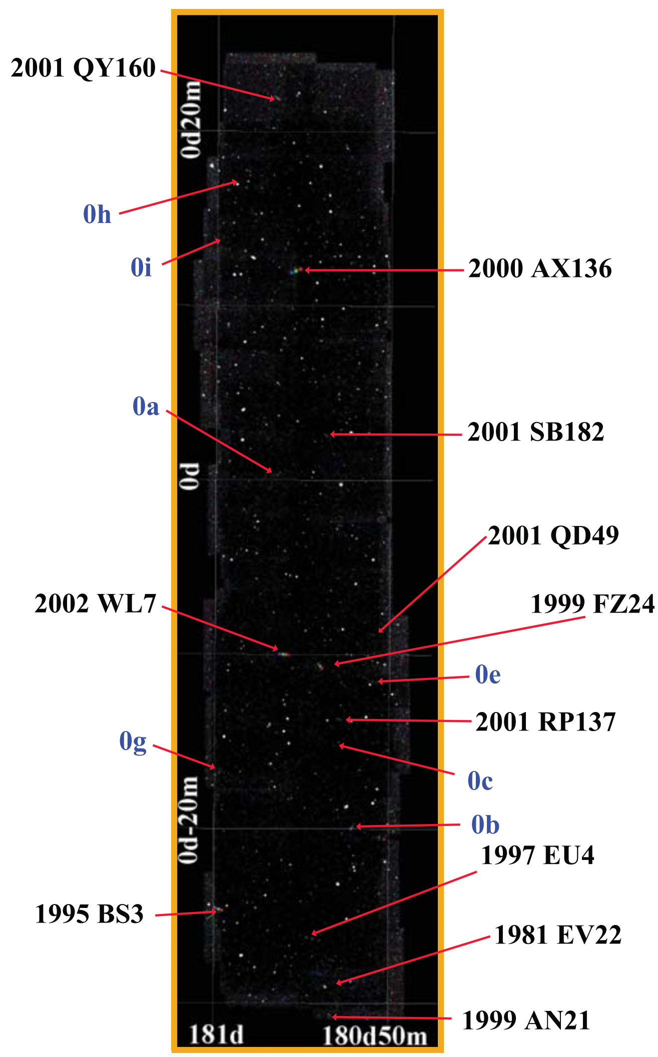

Fig. 1.— IRAC mosaic of the FLS-EPC 0° field. This image shows 3 epochs that have been individually colored, Red, Green and Blue, and coadded. Objects that were stationary over the three epochs appear white. Moving objects can be seen as linear, equally-spaced sequences of red, green and blue sources. Identified asteroids, both known and unknown, are labeled. Note that the asteroids originally designated 0d and 0f, were subsequently identified as 2001 RP137, and 2001 QD49, respectively, after improvements in the ephemeris information.

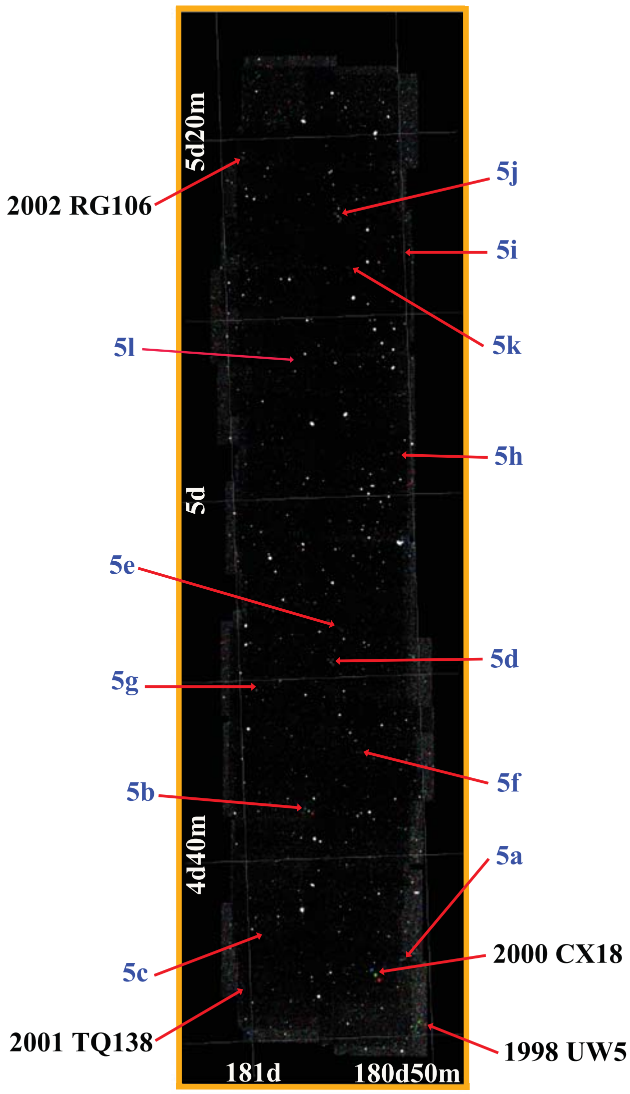

Fig. 2.— IRAC mosaic of the FLS-EPC +5° field, processed as described in Figure 1.

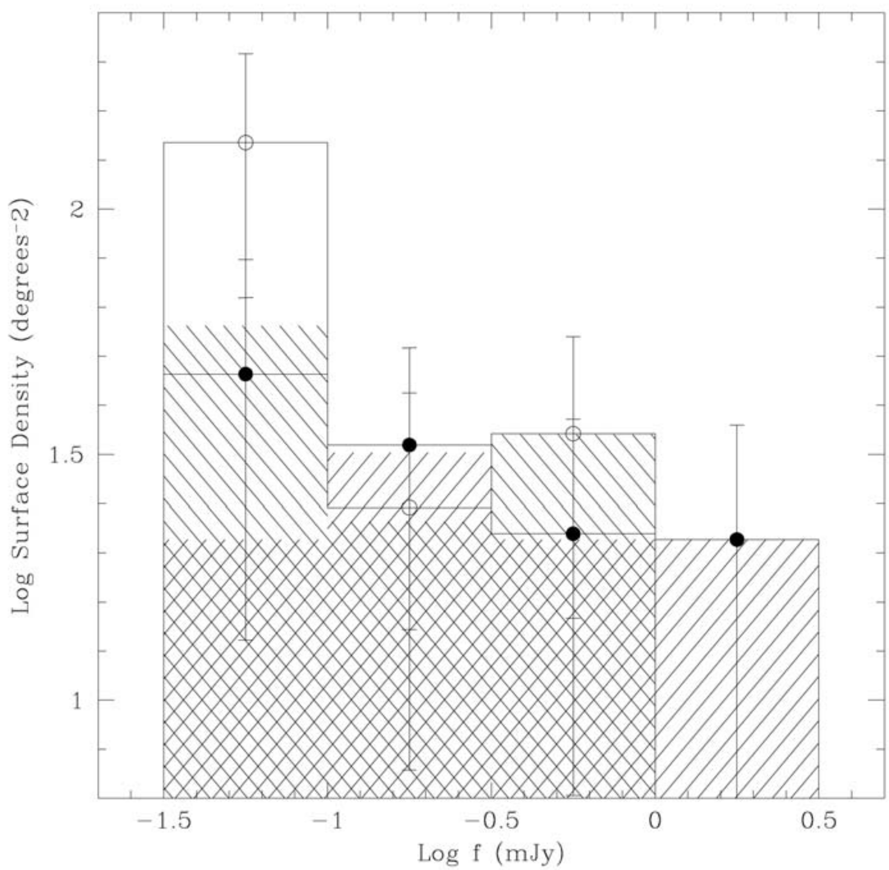

Fig. 3.— Asteroid luminosity functions before and after correction for completeness. The hatched regions show the uncorrected counts, the filled circles show the corrected counts for the 0° field, and the open circles correspond to the corrected counts for the 5° field. The error bars shown reflect both counting statistics and relative errors contributed by the uncertain completeness corrections.

Table 1. MIR Fluxes for Known Asteroids in the FLS-EPC Fields

Asteroids	8μm flux (mJy)	24μm flux (mJy)	Apparent V mag	Absolute H mag
1995 BS3	5.6	41	18.1	13.5
2000 AX136	3.6	30	17.2	13.1
2002 WL7	2.7	23	20.1	15.6
1999 FZ24	2.3	19	19.1	13.8
1981 EV22	1.1	12	19.3	14.0
2001 QY160	0.96	12	20.0	14.9
1998 UW5	0.91	6.9	19.5	15.7
1999 AN21	0.90	11	19.1	14.2
2001 RP137	0.27	2.7	21.8	16.7
1997 EU4	0.20	2.4	20.1	16.9
2001 SB182	0.22	1.9	21.1	15.9
2001 QD49	0.089	1.1*	22.4	17.5

Note. — The uncertainties in these values are conservatively set at 15% for both IRAC and MIPS. Note also that 2001 QD49 was superimposed on a faint background galaxy in the MIPS observation, and conseqently its MIPS flux is likely to be an overestimate

Table 2. Observed and Predicted Asteroid Number Counts

Field	Brooke Pred.	IDAS extrapolation	SAM Pred.	FLS-EPC Observed
0° Field	532	185 ± 38	206 ± 19	154±37
5° Field	236	-	107 ± 21	125±33

Note. — Number counts are per square degree to a 5-σ sensitivity of 0.1mJy. The Brooke (2003) values are considered to be accurate to within a factor of 3